

Development of 3D extended-aperture spatial compounding to improve ultrasound-based localization of the uterus for radiotherapy treatment

Sarah A. Mason

*Joint Department of Physics
Institute of Cancer Research
Sutton, UK
sarah.mason@icr.ac.uk*

Ingrid M. White

*Radiotherapy and Imaging
Royal Marsden NHS Foundation Trust
Sutton, UK
ingrid.white@rmh.nhs.uk*

Tuathan P. O'Shea

*Radiotherapy Physics
Royal Marsden NHS Foundation Trust
London, UK
tuathan.o'shea@rmh.nhs.uk*

Susan Lalondrelle

*Radiotherapy and Imaging
Royal Marsden NHS Foundation Trust
Sutton, UK
susan.lalondrelle@rmh.nhs.uk*

Jeffrey C. Bamber

*Radiotherapy and Imaging
Institute of Cancer Research
Sutton, UK
jeff.bamber@icr.ac.uk*

Emma J. Harris

*Joint Department of Physics
Institute of Cancer Research
Sutton, UK
emma.harris@icr.ac.uk*

Abstract—The aim of this study was to improve uterine target localization in cervix cancer radiotherapy by improving ultrasound image quality. This was achieved through the development of a novel technique called “3D extended-aperture spatial compounding” (3D-EASC), which used the optical probe-tracking technology of the Clarity[®] system to improve ultrasound image quality by extending the field of view, reducing ultrasonic speckle, and enhancing the ultrasound amplitude from tissue boundaries. Changes in image quality due to 3D-EASC were quantified using non-compounded image volumes as a reference in both phantom and in vivo studies. 3D-EASC increased the contrast-to-noise ratio, maintained spatial resolution, and improved the mean observer ranking of image quality of in vivo images of the uterus compared with non-compounded images.

Index Terms—spatial compounding, 3D ultrasound, cervical cancer, image quality, uterus, radiotherapy

I. INTRODUCTION

Poor image quality of current online imaging methods such as cone-beam computed tomography (CBCT) limits the ability to localize soft tissue targets such as the uterus prior to radiotherapy (RT) delivery [1]. Good soft tissue contrast of ultrasound imaging has motivated the development of ultrasound-based radiotherapy guidance systems enabling the spatial registration of ultrasound images to an external reference point in the RT treatment room via probe-tracking technology. The Clarity[®] system (Elekta Ltd. Stockholm) is the latest commercially available ultrasound-guided RT system and uses infrared optical tracking to determine the position of the ultrasound probe with respect to the isocentre of the treatment room [2]. However, low probe-pressure scanning (to minimize internal tissue deformation), operator inexperience, a limited field of view, and inadequate bladder filling can all contribute to the degradation of ultrasound image quality in

the RT clinic making it difficult to identify and segment the uterus in some cases. To address this, a novel method using Clarity's probe-tracking technology was developed to create 3D extended-aperture spatially compounded images. Image quality was evaluated as a function of the number of ultrasound images used to create a compounded image in a phantom and in vivo.

II. MATERIALS AND METHODS

A. Clarity[®] system

The Clarity system includes a Polaris infrared camera (Northern Digital Inc., Waterloo, ON, Canada) mounted in the treatment room which monitors the position of an infrared reflector array attached to a 3D convex mechanically swept probe with a 5 MHz center frequency (model m4DC7-3/40). The Polaris camera can determine the position and orientation (i.e. the rigid body 6D pose) of this reflector array with mean errors and 95% confidence intervals (CI) of 0.19 [0.46] mm and 0.38 [0.71] °, respectively [3].

B. Phantom experiments

A commercial CIRS ultrasound quality assurance phantom (model 040GSE, Universal Medical Inc., Oldsmar, USA) was scanned with the Clarity system to measure the imaging characteristics of compounded and non-compounded images. A room temperature (22°C) salt water stand-off at a concentration of 64 grams per litre was used as the coupling agent between the ultrasound probe and the phantom [4]. The phantom was placed on the treatment couch, and aligned to the lasers according to external markers on the phantom. The ultrasound image acquisition parameters used are shown in Table I.

TABLE I
CLARITY SCANNING PARAMETERS USED TO IMAGE THE CIRS PHANTOM

Center Frequency:	5 MHz
Imaging Depth:	18 cm
Elevational Focus:	6 cm (system default)
Lateral Focus:	6 cm (manually set to match elevational focus)

The Clarity ultrasound probe was clamped in place such that the probe was normal to (but not touching) the phantom surface, and the central scan plane was approximately parallel to the left-right edges of the phantom. The probe was translated seven times in one dimension (1 cm increments) by a motion platform such that the same 4 greyscale targets in the phantom were visible in each 3D image acquired at every probe position. Note that translating the probe enabled insonification of the same targets from different angles because the probe was curvilinear.

C. In vivo experiments

Transabdominal ultrasound scans of the uterus were acquired in four healthy volunteers and four uterine cervix radiotherapy patients at multiple time points. Ethics approval for these studies was obtained from the NHS Research Ethics Committees (reference: 15/LO/1438). Within each scanning session, six ultrasound images (healthy volunteer cohort) or four ultrasound images (patient cohort) of the uterus were acquired from different viewpoints using as little probe pressure as possible within a 5 minute time frame. 21 and 15 scanning sessions were performed for the healthy volunteer and patient cohorts, respectively.

D. Generating 3D-EA spatially compounded images

The 3D ultrasound image stack was interpolated onto a 3D Cartesian grid using the off-line Clarity workstation. These interpolated ultrasound image volumes were spatially registered and re-sampled to a new Cartesian grid of fixed size and position using in-house software written in MATLAB® (Mathworks, Natick MA); these re-sampled 3D-ultrasound images were then averaged together by taking their mean to form a 3D-EA spatially compounded image.

This method can be used to generate image compounds (imCs) from two or more individual ultrasound images. In the case of the phantom, six imCs were generated by combining 2, 3, 4, 5, 6 and 7 individual images. In the healthy volunteer cohort, five imCs were generated by combining 2, 3, 4, 5, and 6 individual images. In the patient cohort, 2, 3, or 4 imCs were generated by combining 2, 3, 4, and 5 individual images.

E. Phantom analysis methods

Contrast-to-noise ratio (CNR): The CNR between four greyscale targets (foreground) and the background of the phantom at the same depth was calculated for all uncompressed imCs and the uncompressed non-compounded images. CNR was calculated as $|\mu_f - \mu_b| / \sqrt{(\sigma_f^2 + \sigma_b^2)}$, where μ is the mean intensity and σ is the standard deviation. A one-way ANOVA test was performed to determine whether the CNR of the four

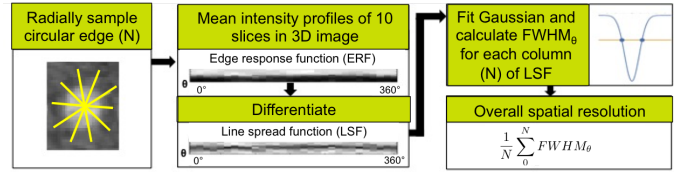


Fig. 1. Schematic indicating how spatial resolution was determined using a hyperechoic target in the CIRS ultrasound quality assurance phantom.

greyscale targets on each imC was significantly different than the CNR on the non-compounded image.

Spatial resolution: In ultrasound imaging, spatial resolution is conventionally described in axial, lateral, and elevational components using the incident beam as a reference. As an imC is comprised of individual images acquired at arbitrary angles, describing resolution using the incident ultrasound beam as a frame of reference is no longer valid. Therefore, the spatial resolution in this work is reported as a single value describing the planar impulse (i.e. the 3D version of a line spread function) of a circular hyperechoic target embedded in the CIRS phantom [5]. Specifically, the intensity profiles along radial samples from 0°- 360° were extracted from the hyperechoic target on 10 consecutive slices in the 3D-ultrasound volume (resampled onto a cartesian grid). The mean intensity profile was calculated along each radial sample to determine the edge response function (ERF). The 3D line spread function (LSF) was then calculated by differentiating the ERF. The spatial resolution was determined by fitting a gaussian (least squares fit) to the LSF of each radial sample: the smaller the full-width-half-maximum (FWHM) of the gaussian, the sharper the boundary between the background and the target, and hence the higher the spatial resolution. The mean FWHM of every radial sample was calculated to represent the overall spatial resolution of the image. This process is illustrated in Figure 1. A one-way ANOVA test was performed to determine whether the spatial resolution of each imC was significantly different to the spatial resolution on the non-compounded image.

F. In vivo analysis methods

Three observers (one clinical oncologist, one radiographer and one medical physicist) independently ranked randomized sets of images (non-compounded and imCs) for image quality of the uterus for both healthy volunteer and patient cohorts. In addition to randomizing the order, the tops of the ultrasound image volumes were cropped to better conceal the level of compounding for each image. In the healthy volunteer cohort where 6 images were compared (the non-compounded image and imCs 2 - 6), rating 1 represented the lowest quality image, and rating 6 represented the highest quality image. In the patient cohort where 4 images were compared (the non-compounded image and imCs 2 - 4), rating 1 represented the lowest quality image and rating 4 represented the highest quality image. Wilcoxon signed-rank tests with bonferroni correction were used to measure differences in mean rank of

3 observers between the imCs and non-compounded images for each cohort.

III. RESULTS

A. Phantom results

Figure 2 shows the non-compounded, the imC comprised of four individual ultrasound images (4-imC), and the 7-imC of the phantom and the CNR for each of the grayscale targets assessed as a function of image compounding.

CNR: 3D-EASCs had a significantly increased CNR in every grayscale target assessed compared with the non-compounded image ($p < 0.05$). The percent increase in CNR ranged from 35% - 255% depending on the nominal contrast of target assessed and the number of individual images comprising the 3D-EASC.

Spatial resolution: There was no difference in the spatial resolution between any of the imCs and the non-compounded image as measured by the FWHM of the 3D LSF ($p = 0.89$, mean = 1.38 mm). However, Figure 2 demonstrates that there was a visual improvement in the spatial resolution of the wire targets.

B. In vivo results

Figure 3 demonstrates the change in ultrasound image quality of the uterus as a function of 3D-EASC. In cases where the non-compounded ultrasound image was of low quality, 3D-EASC improved the visibility of the uterus by increasing the contrast between the uterus and the background, and by enhancing edges - particularly at the uterus-bladder interface and the posterior border of the uterine body. In cases where the non-compounded ultrasound image was already of high quality (Figure 3, Patient 4) compounding extended the field of view, and reduced speckle. Non-compounded images had significantly poorer mean rankings than all imCs in both the healthy volunteer and patient cohorts as measured by the Kruskal Wallis test ($p < 0.05$). Furthermore, the mean rank was significantly improved with increasing levels of compounding ($p < 0.05$), with the exception of the last two most heavily compounded images and the 3-imC and 4-imC in the volunteer cohort, in which there was no difference, as shown in Figure 4.

IV. DISCUSSION

The results from the phantom experiment demonstrate that 3D-EASC can improve the CNR in ultrasound imaging without degrading the spatial resolution. Indeed, the appearances of the wire targets in the phantom suggest that 3D-EA spatial compounding may produce a small improvement in spatial resolution. This is because different viewpoints of the same object can be achieved by physically moving the probe to any desired position in 3D-EASC rather than splitting the array into sub-apertures. This not only makes it easier to acquire images with statistically independent speckle to maximize CNR improvements [6], but also preserves the lateral resolution of the system as the aperture length not reduced.

Results from the observer ranking study indicate that the observers perceive image quality to be better on imCs compared with non-compounded images. This was expected given the theoretical improvements in image quality offered by spatial compounding [6]–[8] and the promising results from the phantom experiment. Although we did not reach a point where 3D-EASC negatively impacted the overall image quality, the benefit of 3D-EASC appeared to reach a maximum, whereby the perceived image quality stopped improving after compounding more than 3 and 5 ultrasound image volumes for patients and volunteers respectively. This could be due to the balance between competing factors of (a) increased magnitude and likelihood of edge blurring due to probe-pressure induced tissue deformation or natural physiological motion and (b) the continuing increase in CNR. It could also be due to the fact that the pelvic bones limit the acoustic window such that only a few probe orientations provide independent viewpoints of the uterus. Even in the presence of these challenges, 3D-EASC provided significant improvements in image quality compared with non-compounded images in addition to extending the field of view.

V. FUTURE WORK

3D-EASC provides a rare opportunity to improve ultrasound image quality at virtually no cost; the optical tracking hardware is already in place, the computation time for generating image compounds is small (< 1 minute), and it only takes an additional minute or two of additional ultrasound scan time to acquire multiple ultrasound image volumes. One aspect of 3D-EASC that was not directly explored in this work was how positioning the elevational focal point in different positions affected the spatial resolution. Although this was done in practice in the in vivo scans, the phantom experiments were designed to measure the image specifications as a function of 2D compounding rather than 3D largely because the phantom is 2D not 3D (i.e., it contains wires and cylinders, not points and spheres). To measure the potential improvement in resolution offered by 3D-EASC, the phantom experiment could be repeated, but with the phantom rotated by 90° to enable the acquisition of the same 4 greyscale targets from different image planes.

Also, the current implementation of 3D-EA spatial compounding weights all of the individual voxels comprising the compound equally. The next step would be to devise a way of identifying regions where ultrasound image quality is degraded such that they could be removed or penalized to reduce the influence of artefacts in the compounded image. For example, it may be possible to adapt the multiple-receive and crossbeam filtering techniques developed by Li and O'Donnell (1994) to eliminate unwanted sidelobes resulting from blocked acoustic elements using the ultrasound images themselves [9]. Similarly, it could be possible to characterize the ultrasound signal in terms of its spatial frequency components along each a-line to detect artefacts arising from obstructions in the beam path or poor probe contact such that the contribution of these voxels to the final image is reduced or eliminated.

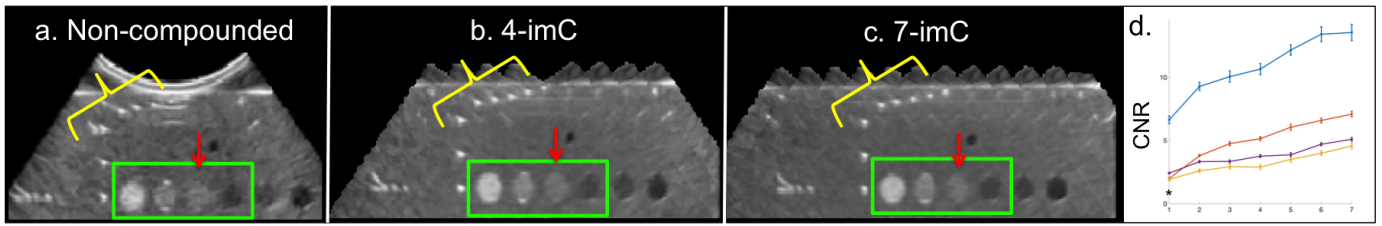


Fig. 2. a - c: Example ultrasound frames from the non-compounded image, the 4-imC, and the 7-imC. The CNR was quantified for each grayscale target (>15dB, 6 dB, 3 dB, and -3 dB from left to right) in the green box. Note the improved visibility of the 3 dB target (red arrow) with 3D-EASC. Also note the improved resolution of the wire targets (yellow bracket). d: plot showing the CNR for each grayscale target. The blue, orange, purple, and yellow lines represent the >15 dB, 6 dB, 3 dB, and -3 dB targets, respectively.

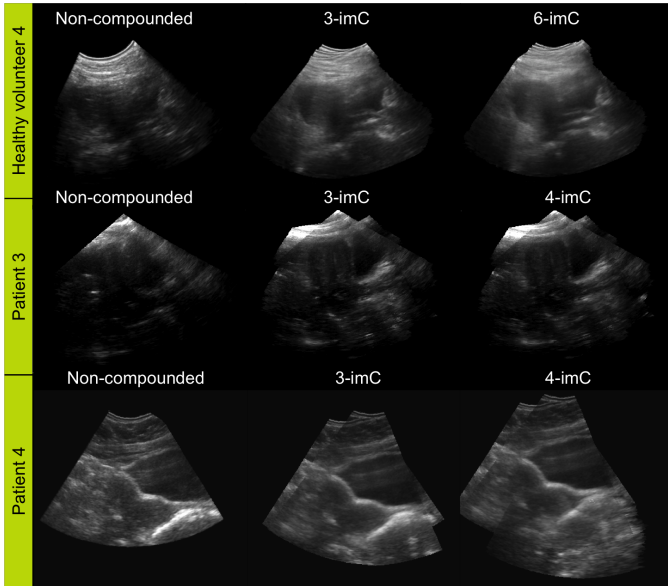


Fig. 3. The same sagittal frame of the uterus shown for the non-compounded image and 2 - 6 imCs for one healthy volunteer (row 1) and two cervical cancer patients (rows 2 and 3).

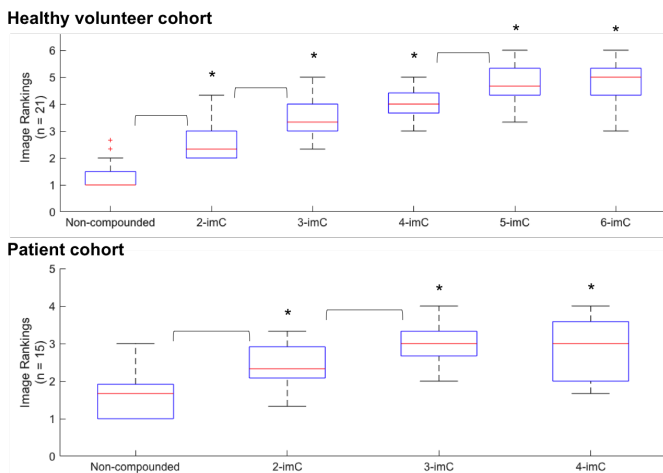


Fig. 4. Boxplots showing the mean rank from 3 observers indicating image quality (1 = poorest quality). All imCs had significantly higher mean ranks than the non-compounded image in both the healthy volunteer and patient cohorts as indicated by the * symbol ($p < 0.05$). Brackets indicate significant differences in mean rank between neighboring imCs ($p < 0.05$).

VI. CONCLUSIONS

3D-EASC offered significant improvements in CNR without degrading spatial resolution in vitro. When compared side-by-side with non-compounded images, observers consistently ranked imCs higher than non-compounded images in terms of image quality of the uterus. 3D-EASC using the Clarity system could therefore be used to improve ultrasound image quality such that the uterus can be quickly and accurately localized for the purpose of guiding and/or adapting radiation treatment for cervical cancer patients.

ACKNOWLEDGMENTS

The authors would like to acknowledge Helen McNair and Matthew Blackledge for participating as observers in this study.

REFERENCES

- [1] M. Baker, J. A. Jensen, and C. F. Behrens, "Determining inter-fractional motion of the uterus using 3D ultrasound imaging during radiotherapy for cervical cancer," *Proc. of SPIE*, vol. 9040, pp. 90400Y–90400Y–10, 2014.
- [2] M. Lachaine and T. Falco, "Intrafractional prostate motion management with the Clarity Autoscan system," *Medical Physics International*, vol. 1, no. 1, pp. 72–80, 2013.
- [3] A. D. Wiles, D. G. Thompson, and D. D. Frantz, "Accuracy assessment and interpretation for optical tracking," in *Proceedings of SPIE 5367, Medical Imaging 2004: Visualization, Image-Guided Procedures, and Display*, 2004.
- [4] A. B. Coppens, "Simple equations for the speed of sound in Neptunian waters," *The Journal of the Acoustical Society of America*, vol. 69, no. 3, 1981.
- [5] S. W. Smith, *The Scientist and Engineer's Guide to Digital Signal Processing*. San Diego: California Technical Publishing, 1997.
- [6] P. M. Shankar, "Speckle reduction in ultrasound B-scans using weighted averaging in spatial compounding.," *IEEE transactions on ultrasonics, ferroelectrics, and frequency control*, vol. 33, no. 6, pp. 754–758, 1986.
- [7] S. K. Jespersen, J. E. Wilhjelm, and H. Sillesen, "Multi-Angle Compound Imaging," *Ultrasonic imaging*, vol. 20, no. 2, pp. 81 – 102, 1998.
- [8] D. E. Robinson, "Digital Reconstruction and Display of Compound Scan Ultrasound Images," *IEEE Transactions on Sonics and Ultrasonics*, vol. 31, no. 4, pp. 396–406, 1984.
- [9] P. C. Li and M. O'Donnell, "Efficient two-dimensional blocked element compensation.," *Ultrasonic imaging*, vol. 16, pp. 164–75, jul 1994.